Original Article

Design And Characterization Of Barberine Liquisolid Compacts For Escalating Bioavailability And Antidiabetic Potential :In Vitro,In Vivo And In Silico Approach

Mohan D.Dhere[1*], E.Bhavya[2]**

[1] Department of Pharmacy Practice, Vels University,Pallavaram, Chennai, India.
[2] Ph.D Research Scholar, Vels University, Pallavaram, Chennai, India Email ID: mohan.dhere@rediffmail.com

Corresponding Author
E.Bhavya Vels University,Pallavaram, Chennai, India Email ID:bhavyavivek24@gmail.com
DOI: 10.47750/pnr.2022.13.S09.1098

Abstract

The current investigation aimed to develop a barberine (BRN) loaded liquidsolid compact (SLC) to improve the oral therapeutic effectiveness of BRN. 3^2 full factorial design was employed and the effect of the carrier:coating ratio (X1) and neusilin :corn starch ratio (X2) was systematically investigated on percentage cumulative drug release (Y1) and disintegration time (Y2). In total, 09 experimental runs (SLC–1 to SLC–9) were prepared, evaluated, and converted to solid free-flowing granules using neusilin® US2. SLC–6 comprising labrasol and neusilin : corn starch ratio 8:2 quick disintegration time 58.54±2.59 sec. and higher cumulative drug release 98.12±2.53. FT-IR spectra showed no incompatibilities, whereas DSC results confirmed the amorphous state and molecular dispersion of BRN in liquidsolid compact. In vitro dissolution studies demonstrated significant ($P<0.05$) improvement in BRN release characteristics from BRN liquidsolid compact (SLC–6). In-silico studies confirmed hydrogen bond interaction between an oxygen group of BRN and neusilin hydrogen. SLC–6 showed significant ($P<0.05$) antidiabetic activity when compared to pure BRN and standard acarbose conformed by α-amylase inhibitory and α-glucosidase inhibitory Assay. Remarkably, a 8-fold increase in bioavailability was observed after oral administration of BRN LSC–6 than plain BRN. Thus, BRN liquidsolid compact could be utilized as a potential carrier for BRN delivery in treatment of diabetis.

Keywords: Liquidsolid Compact, Barberine, Antidiabetic, In-silico study, Bioavalability etc.

1. Background

Diabetes mellitus is a chronic disease caused by a partial or total deficiency of insulin, which causes hyperglycemia leading to acute and chronic complications [1]. The incidence of diabetes mellitus is increasing worldwide. Control of plasma glucose concentrations is vital for decreasing the incidence and severity of the long-term effects of diabetes [2].Diabetes is a major cause of blindness, kidney failure, heart attacks, stroke and lower limb amputation.[3] About 422 million people worldwide have diabetes, the majority living in low-and middle-income countries, and 1.5 million deaths are directly attributed to diabetes each year. Both the number of cases and the prevalence of diabetes have been steadily increasing over the past few decades.[4]

The poor dissolution rate, water solubility and low bioavailability of the drugs is still a substantial problem confronting the pharmaceutical industry in treatment of diabetis. A great number of new and, possibly, beneficial chemical entities do not reach the market merely because of their poor oral bioavailability due to inadequate dissolution.[5] Over the years, various solid dosage formulation techniques to enhance the dissolution of poorly soluble substances have been introduced with different degrees of success. The technique of 'liquisolid compacts' is a new and promising addition towards such a novel aim. [6]

It is well established that the active ingredient in a solid dosage form must undergo dissolution in order to become available for absorption from the gastrointestinal tract. The absorption rate of a poorly water-soluble drug, formulated as an orally administered solid dosage form, is controlled by its dissolution rate in the fluid present at the absorption site, i.e. the dissolution rate is often the rate-determining step in drug absorption. [7] Liquisolid technique is a new and promising method that can change the dissolution rate of drugs. Ithas been used to enhance dissolution rate as well as bioavalabilty of poorly water-soluble drugs.[8] For BCS Class II drugs, the rate of oral absorption is often controlled by the dissolution rate in the gastrointestinal tract. Therefore, together with the permeability, the solubility and dissolution behavior of a drug are key determinants of its oral bioavailability. [9]

Berberine (BRN) is an isoquinoline alkaloid mainly used to treat diabetis, hypertension and inflammatory conditions.BRN has also been reported to have a number of pharmacological actions including anti-malarial, anti-arrhythmic, anti-hyperglycemic, anticancer, hepato-protective, antioxidant, and antimicrobial.[10] However, the poor water solubility of BRN impacts its dissolution rate and oral bioavailability, thus limiting its clinical use.[11] BRN appears to be a hydrophilic compound and has a log P-value of -1.5,32 which makes BRN a class III drug in the biopharmaceutical classification system (BCS). Drugs included in this class are lipophobic and have poor membrane permeability, and the absorption of the drugs is mostly limited to the paracellular pathway. This limits intestinal absorption and leads to low bioavailability.[12]

Liquisolid dispersion technique has been widely used to improve the dissolution and bioavailability of poorly water-soluble drugs with a low dose [13]. A liquisolid formulation allows an insoluble drug to be solubilized, almost molecularly dispersed in a solid dosage form, which greatly enhances the dissolution rate of solubility-limiting drugs due to ameliorative wetting property and dissolution surface area, hence the oral bioavailability.[14]

Recently numerous lipophilic and poorly water soluble drugs such as efavirenz [15], Telmisartan [16], lovastatin[17], Chlorpromazine [18], Glyburide [19], Glimepiride [20],Rosuvastatin [21], Fenofibrate [22] etc. have been formulated into liquidsolid compact to accomplish enhanced therapeutic efficacy.

Therefore, an attempt has been made to design and optimize the liquisolid compacts to enhance in– vitro and in-vivo antidiabetic efficacy of BRN via the oral route. Herein, formulation optimization was done using a two-factor, three-level (3^2) full factorial design. Optimized liquisolid compact was evaluated for different parameters such as flowability, crystallinity, in-vitro drug release, etc. Afterward, in-silico interactions, in-vitro antidiabetic potential and in-vivo pharmacokinetic studies were performed

2.Materials and Methods

Barberine was procured from Sigma aldrich Pvt. Ltd. Mumbai, India. Labrasol, Kolliphor, Kollisolv and Cremophor-RH-40, were gift samples given to us by Gattefosse in Mumbai, India. Fuji Chemicals Japan has been kind enough to send over a sample of Neusilin US2 as a present. We purchased Tween 20, Tween 80,PEG 400 and double-distilled water from Unique Chemicals in Kolhapur, India. In this research, analytical-grade chemicals have been utilized.

2.1. Solubility Studies

The phase solubility strategy was applied in the conduct of the experiment concerning solubility. In a brief, an excessive amount of BRN was put into separate test tubes, each of which contained 2 milliliters of different lipids as given in Table 1. Resultant mixtures have been shaken at 37°C for 24 h using Orbital Shaker (Remi, RIS-24 Plus, and Mumbai, India). After equilibrium, each sample has been centrifuged (Remi, RM-12C, India) for 15 minutes at 2000 rpm. Then, after the clear supernatant has been filtered through a membrane with a pore size of 0.45 micrometres, absorbance readings were taken with a spectrophotometer (Shimadzu-1900, Japan) that measures UV and visible light at 348 nm [23].

2.2.Preparation of BRN liquisolid compact.

Method for formulating liquisolid compact The required amount of the BRN and non-volatile co-solvent were added in 20 ml glass beaker and heated gradually until all the SGN was solubilized. The resultant warm liquid medication was incorporated into the fixed amount of carrier and coating materials initially, the powder excipient and liquid medicaments were blended at an estimated mixing rate of one rotation per second for nearly one minute in order to have a uniform distribution of the liquid medication in the powder. Liquid/powder admixture was evenly spread as a uniform layer on the surfaces of a mortar and left standing for approximately 5 min to allow the drug solution to get absorbed in the internal matrix of the powder material. Further,

the powder is scraped off from the surface of mortar by using an aluminum spatula and then mixed with the disintegrating agent for another 30 seconds in the same way described earlier. The yielded final liquisolid formulation was compressed in tablet form [24].

2.3.Experimental design

A two-factor, 3-level (3^2) factorial design for Saxagliptin-liquisolid tablet (BRN-LSC) was used for the optimization of the liquisolid compact formulations where the two factors were evaluated each at three different levels (low, medium and high) and experimental trials were performed using all possible nine combinations using the Software: Design Expert software (Version 7.0.0, Stat-Ease Inc., USA). The Independent variables chosen for liquisolid compact were the percentage of Carrier: Coating Ratio (X_1) and (Neusilin:Corn starch Ratio) (X_2) whereas Drug Release (Y_1), and Disintegration Time (Y_2) were selected as the dependent variable. Amount of BRN was kept constant (50 mg) in all batches for the preparation of the liquisolid compact. The independent and dependent variables used in the 3^2 factorial design approach for the formulation of BRN liquisolid compact are shown in Table 1.

Table 1.Full factorial Design matrix summarizing the levels, factors, and responses of 09 runs for optimization of BRN liquisolid compact.

Run	Block	Factor 1 Carrier :Coating Ratio	Factor 2 (X2) (Neusilin : Corn starch Ratio) (R value)	% Cumulative Drug Release (Y1)	Disintegration Time in Seconds (Y2)
1	BRN LSC-1	10 (-1)	9:1 (-1)	58.23±3.73	84.32±7.16
2	BRN LSC-2	20 (0)	9:1 (-1)	67.57±3.32	77.54±6.26
3	BRN LSC-3	30 (1)	9:1 (-1)	72.98±4.72	73.65±4.32
4	BRN LSC-4	10 (-1)	8:2 (0)	80.43±2.95	69.42±4.38
5	BRN LSC-5	20 (0)	8:2 (0)	87.12±2.32	66.65±3.27
6	BRN LSC-6	30 (1)	8:2 (0)	98.12±2.53	58.54±2.59
7	BRN LSC-7	10 (-1)	7:3 (1)	83.31±3.16	64.22±3.47
8	BRN LSC-8	20 (0)	7:3 (1)	85.38±3.64	60.12±2.05
9	BRN LSC-9	30 (1)	7:3 (1)	91.43±2.05	56.62±1.24

Factor	Levels used, actual (coded)		
	Low (-1)	Medium (0)	High (+1)
Independent variables			
Factor 1 (X1) **(Carrier :Coating Ratio)**	10	20	30
Factor 2 (X2) **(Neusilin : Corn starch Ratio)**	9:1	8:2	7:3
Dependent variables			
Drug Release (Y1)	**Maximize**		

Disintegration Time (Y2)	**Minimize**

2.4.Mathematical model for designing SGN liquisolid Compact

Spireas and Bolton have introduced a mathematical model for producing liquisolid compacts with acceptable flowability and compactibility. This model is based on the hypothesis that powder material can only accommodate a specific amount of liquid medicament (co-solvent + drug) in the inner matrix while preserving acceptable flowability and compatibility. Once the proportion of liquid exceeds the certain limit, the flow property and compactibility of the powder material starts to decline. This maximum amount of liquid which a powder material can retain while maintaining acceptable flowability and compatibility is known as flowable liquid-retention potential (Φ – number) and compressible liquid-retention potential (Ψ – number) respectively. The acceptable compactibility means the ability of powder material to produce cylindrical compacts of adequate crushing strengths (approximate 5–6 kg/cm2) and acceptable friability without presenting any ‘‘liquid-squeezing - out” phenomena during compression. Once the inside matrix is saturated with liquid medication, the extra liquid will start to deposit as a layer on the surface of powder material. This extra layer of liquid is adsorbed by adding another powder excipients known as ‘‘coating material” that finally leaves the total powder material free-flowing, non-adherent and compressible. ‘‘Excipient Ratio” (R) is defined as the ratio of carrier and coating material required to make powder with acceptable flowability and compressibility.[25]

$R = Q/q$ [1]

where Q = amount of carrier material and q = amount of coating material.

2.4.1.Determination of flowable liquid-retention potential (Φ – value)

The liquid medicament was gradually added to the fix quantity powder material (10 gm) and this resulted admixture was placed at one end of the polished metal plate. The metal plate was gradually uplifted from one side while keeping the other side on the ground. The angle formed between plate and ground was consid ered as the angle of slide [26]. The angle of slide value of around 31 represents the optimal flowable property of powder excipient with respect to the particular liquid vehicle used. [27]

2.4.2.Determination of compressible liquid-retention potential (Ψ – value)

The liquid medicament was added gradually to 1 gm powder material for making uniform admixture. The admixture was compressed with specific hardness in the rotary tablet machine to make a tablet. In this investigation, the crushing strength value between 5 and 7 Kgf was considered as an acceptable one. During compression, it was also observed that there was no leakage of liquid medicament from the powder admixture [28]

2.4.3.Liquid load factor

Once Φ – value and Ψ – value of carrier and coating material was measured, the liquid load factor for acceptable flowability and compressibility was calculated by using the following equations.

$\Phi Lf = \Phi CA + \Phi CO\ [1/R]$ for flowability [2]

$\Psi Lf = \Psi CA + \Psi CO\ [1/R]$ for compressibility [3]

Here Φ CA and Φ CO are flowability liquid retention potential of carrier and coating materials respectively and Ψ CA and Ψ CO are compressible liquid retention potential of carrier and coating materials respectively. R is the excipient ratio as defined by Eq. (1). According to studies published in different research articles, it was noted that the R-value between 10 and 20 resulted in optimal flow property and acceptable compactible property so in this investigation a mean of 15 was taken for calculation [29]

The liquid load factor can also be calculated by using the weight of liquid and carrier material as per the following equation.

$Q = W/Lf$ [4]

Q = Weight of carrier material and W = Weight of liquid medicament.

Here between Φ Lf and Ψ Lf whichever had the lower value was put in Eq. (4). Eq. (4) gave the weight of carrier material required to imbibe particular liquid medicament. The obtained value of Q was applied in Eq. (1) to calculate the value of the coating material required to adsorb the extra liquid layer from the surface.

2.4.4.Primary trial for selection of carrier and coating material.

The primary trials were conducted to identify the carrier and coating material which can accommodate maximum liquid medicament without losing flowability and compactibility. The methods used for screening are described in the abovementioned

section under the heading of ‘‘Determination of Flowable liquid-retention potential” and ‘‘Determination of compressible liquid-retention potential”. The obtained values were put in Eqs. (3) and (4) for calculating the liquid loading factor.

2.5.Preformulation Studies

2.5.1.Bulk Density and Tapped Density

BRN liquisolid compact powder (n=3) of weight 'W' was transferred to a graduated cylinder (100 mL) and noted the initial volume (Vb). Afterward, we used bulk density apparatus (Lab Hosp, Mumbai, India) to tap the sample until the constant volume (Vt) has been reached. The tapped density (TD) and bulk density (BD) have been calculated as follows [30],

$$\mathrm{BD} = \frac{\mathrm{W}}{\mathrm{Vb}} \qquad \text{Eq. 5}$$

$$\mathrm{TD} = \frac{\mathrm{W}}{\mathrm{Vt}} \qquad \text{Eq. 6}$$

2.5.2.**Carr's Index (CCI) and Hausner's ratio (HR)**

CCI and HR were determined in triplicates as follows,

$$\mathrm{CCI} = \frac{(\mathrm{TD} - \mathrm{BD})}{(\mathrm{TD})} \times 100 \qquad \text{Eq. 7}$$

$$\mathrm{HR} = \frac{(\mathrm{TD})}{(\mathrm{BD})} \qquad \text{Eq. 8}$$

2.5.3.**Angle of Repose (θ)**

Fixed-funnel technique was used for estimation of the angle of repose. In brief, BRN liquisolid compact powder was passed through a funnel which produce the heap of which height 'H' and radius 'R' was determined. Below mentioned the formula utilized to calculate the angle of repose [30]

$$\theta = \mathrm{Tan}^{-1}\left(\frac{\mathrm{H}}{\mathrm{R}}\right) \qquad \text{Eq. 9}$$

2.5.4.Fourier transforms infrared (FTIR) spectroscopy

FTIR spectrum of pure BRN, labrasol, neusilin, and the optimized BRN liquisolid compact was recorded using a Bruker, Alpha-T FT-IR spectrophotometer over the frequency range of 4000 to 650 cm^{-1}.[31]

2.5.5.Differential scanning calorimetry (DSC)

DSC thermogram of pure BRN, maisine, neusilin, and the optimized BRN liquisolid compact was measured by a DSC-60 calorimeter (Shimadzu, Japan). The accurately weighed sample was placed onto the aluminum pans and sealed. The sample was heated over the entire range of temperature range 0 °C to 400 °C at an increment of 10 °C /min [32].

2.6.In-Silico Interaction Studies

To explore the bonding and non-bonding interactions of barberine with Neusilin excipient, molecular docking was performed using AutoDock4.2.1. The atomic coordinates of barberine and Neusilin were generated and optimized using the Discovery Studio Visualizer [33,34]. Here, we used blind docking approach similar to earlier studies [23], to understand the interactions of barberine with Neusilin.For docking, the entire Neusilin molecule was enclosed in a grid box of 60×60×60with a grid spacing of 0.375 Å.

Here, we keep the Neusilin rigid and the drug compoundas a flexible molecule.The Lamarckian Genetic Algorithm (LGA) was employed with the default parameters [35]. During the blind docking, at each time Saxagliptin were placed at the random location, and each docking run consists of 100 runs. [36,37]. Thisoutput docked conformation was further clustered using all-atom root means square deviations with a cut-off of 4 Å, similar to an earlier study [23]. The least energy docked conformations were further considered for investigation of bonding and non-bonding interactions analysis using Discovery Studio visualize[38-39].

2.7.1. Dug content

10 BRN liquisolid compact that had been accurately weighed and after being crushed added to the appropriate quantity of methanol and then dispersed. After separating the clear supernatant, the sample has been analyzed spectrophotometrically at 211 nm using a membrane filter with a pore size of 0.45 micrometers. (Shimadzu UV-1900) [40].

2.7.2 Friability Test

The test was performed using Roche friabilator (Electrolab).

2.7.3. Hardness

The hardness of the tablets was determined using Monsanto hardness tester. It is expressed in kg/cm2 . Six tablets from each formulation were tested for hardness.

2.7.4 In-Vitro Disintegration Time

The disintegration time of the tablets was measured in distilled water (37 ± 2°C) using disintegration test apparatus (Electrolab, India) with disk. Five tablets from each formulation were tested for the disintegration time calculations.[29]

2.7.5.In-Vitro Drug Release Study

The in vitro drug release study of the tablets was performed using USP type II apparatus paddle (EDT-08Lx Electrolab) at 37°C ± 0.5°C using phosphate buffer pH 6.8 (900 mL) as a dissolution medium and 50 rpm. At the predetermined time intervals, 5 mL samples were withdrawn and replaced with fresh dissolution media. Withdrawn samples were filtered through a 0.45 micrometer membrane filter, diluted, and assayed at 211 nm using a Shimadzu-1900 UV spectrophotometer. [41]

2.8.In vitro antidiabetic study

2.8.1.α-amylase inhibitory Assay

In a an appendorf tube, 1ml of PBS solution was mixed with 0.5 ml of different concentrations (50, 100, 150, 200 & 250 µg/ml) of samples with the standard solution and 200µl of 0.5mg/ml α-amylase was added followed by 200µl of 5mg/ml starch solution and incubated for 10 minutes at room temperature. Control was takes as starch with amylase and without amylase. Then the reaction mixture was stopped by adding 400µl of DNS solution heating the mixture in boiling water bath for 5 min and cooled. The absorbance was measured at 540 nm (Labman UV Visible Spectrophotometer). Acarbose was used as standard.[42] The percent of enzyme inhibition was calculated using the following formula: % of α-amylase inhibition = $[(Ac - As)/Ac] \times 100$

where, Ac and As are the absorbance of control and sample, respectively.

2.8.2.α-Glucosidase inhibition assays

The assay of α-glucosidase inhibition activity performed as described by Li et al., 2005. ρ-Nitrophenyl-ρ-D-glucopyranoside (PNPG), was used as substrate and prepared by dissolving in 50 mM phosphate buffer (pH 6.5). Samples were prepared at the concentration of 50, 100, 150, 200 and 250 µg/ml dilution method (in 5% DMSO). 30 µL of each concentration was added with 36 µL phosphate buffer pH 6.8 and 17 µL p-nitrophenyl-α-D-glucopiranoside (5 mM). The mixture solution was incubated for 5 min at 37°C. To this solution, 17 µL of α-glucosidase 0.15 unit/mL was added after the first incubation, then incubated again for 15 min at 37°C. After the second incubation was finished, 100 µL of Na_2CO3 267 mM was added into the solution to stop the enzymatic reaction. Solution absorbance was measured with a microplate reader (BIOBASE) at 405 nm. The blank solution was tested by adding Na2CO3 right after the first incubation and α-glucosidase after the second incubation. Ascarbose was tested as positive control. [43] The inhibition percentage was calculated by following formula. The concentration of samples that inhibited α-glucosidase activity by 50% was defined as the IC_{50} value.

Inhibition Percentage= OD of Control-OD of Sample/OD of Control X 100

2.9.In Vivo Pharmacokinetic Study

The experimental protocol (BIRD/CPCSEA/IAEC/Sangli/2022-23/06) was approved by the Institutional Animal Ethics Committee (IAEC) BIRD, Sangli. Wistar albino rats (n=9) weighing in between 180-220g were procured from Crystal biological solution, Pune, India. Different pharmacokinetic parameters have been investigated after oral administration of pure SGN as well as optimized BRN liquisolid compact (BRN LSC-6) to the experimental animals. The animals were kept on a standard supplemented diet and water for two weeks before the experimentation. A random selection was used to divide the rats into three groups. Group, I served as a control, while group II and group III have been designated as test and standard groups. Group I have been administered with physiological saline solution. Optimized SLC at an equivalent dose of BRN (5 mg/kg) has been given orally to the group II animals whereas, group III was administered with BRNdispersed in a 0.5 % sodium carboxymethyl cellulose at 5mg/kg.

After the administration of the dose, blood samples of approximately 500 microliters each were drawn from the retro-orbital plexus of rats and placed into heparinized polyethylene tubes at predetermined intervals (24, 12, 10, 8, 6, 4, 2, 1, and 0.5 h). Plasma obtained from blood samples that have been drawn and processed through centrifugation at 7000 rpm for ten minutes was then frozen at -20 °C for use in subsequent experiments. The validated HPLC strategy was applied to determine the BRN concentrations in the plasma samples that were isolated. Pharmacokinetic parameters, including the C_{max} (maximum plasma concentration), T_{max} (time it takes to reach C_{max}), $AUC_{0-\infty}$ (area under the plasma concentration-time curves), $AUMC_{0-\infty}$ (area under the moment curve), and MRT (Mean Residence Time), has been estimated. [23].

2.10. Stability study

Following ICH recommendations, a stability study has been performed. It was kept in a stability chamber at a temperature of 40 ± 2 °C and 75 ± 5% RH for 90 days. Different parameters like drug content (%) and cumulative drug release (% CDR) were examined at specified time intervals (1, 2 and 3 months) [44]

3. Results and Discussion

3.1. Solubility Studies

BRN solubility was calculated to select the suitable vehicle that can potentially solubilize the BRN in lesser quantity. Liquisolid compact with the appropriate lipids solubility and provides better drug entrapment. Solubility of BRN in lipids was found to be 15.43±1.54 to 172.14 ±3.78 mg/mL and 3.87±0.2. Maximum solubility was found in labrasol (38.54±3.78 mg/mL). Detailed results of solubility studies are shown in Table 2.

Table 2: Solubility of Barberine in Lipids

Vehicles	**Particulars**	**Solubility (mg/mL)***
Solvent	Labrasol	172.14±6.14
	Propylene Glycol	15.23±1.54
	PEG-400	7.22±1.23
	PEG-200	3.16±1.76
	Kolliphor	14.65±0.8
	Kollisolv	12.54±1.10
	Cremophor RH40	8.43±0.6
	Tween 20	4.76±2.47
	Tween 80	5.51 ±2.12

***Each value represents mean ± SD of three observations**

Among all the carrier materials screened, Neusilin had the highest flowable liquid retention potential of 1.2 ml. This meant that 1 gm of Neusilin powder was able to retain its good flow property even after accommodating 1.2 ml of liquid medicament with it (angle of slide = 31). This was followed by compressil 101, fujicalin and microcrystalline cellulose respectively, thus Neusilin was selected as carrier material. (Fig. 2). Among all the coating materials tested, aerosil had the highest flowable liquid retention potential of 1.6 ml. During initial the dissolution studies, it was observed that the liquisolid compacts containing only Neusilin as

carrier material were not able to release the drug completely. This was possibly because of the BRN was entrapped firmly in the internal matrix of Neusilin. To overcome this problem corn starch was mixed with Neusilin. Starch is widely used as a disintegrating agent in tablets because of its swelling property. The swelling property of starch was expected to help the drug to get released easily from the high internal surface area of Neusilin. [45]. The angle of slide was again measured for three newly prepared mixtures of corn starch and Neusilin with the ratios of 1:9, 2:8 and 3:7. It was practically observed that corn starch and Neusilin US2 in the ratio of 1:9, 2:8 and 3:7 had the same liquid retention potential as for plain Neusilin (1.2 ml). In the subsequent trials it was also observed that as the proportion of corn starch was further increased in the mixture, the liquid retention potential started to decrease drastically so it was decided to use Neusilin /corn starch mixture as the carrier material in the ratio of 1:9, 2:8 and 3:7.

Determination of compressible liquid-retention potential

During the compressibility test, it was observed that Neusilin /corn starch in the ratio of 1:9, 2:8 and 3:7. Was able to retain 1.4 ml of labrasol without presenting any leakage problem and were also able to provide acceptable hardness.

Liquid load factor

The liquid load factor was calculated by using Eqs. (2) and (3). As described in the previous section, the U – value and W – value for Neusilin /corn starch (9:1, 8:2 and 7:3) were taken as 1.5 ml. For the selected coating material, aerosil 200 obtained U – value for was 1.8. The R-value as described in the introduction part was taken as 15. By putting all these values in equation (3) and (4), the calculated value of ULf and WLf were found to be 1.6 and 1.4 respectively. Since the WLf < ULf, the value of WLf was finally considered as a liquid load factor for this particular liquisolid system.

Determining the weight of liquid medication

The practically measured solubility of BRN in labrasol was found to be 43.32 mg/ml. To dissolve 50 mg of BRN , 290.46 mg of labrasol was required which led to the total weight of liquid medicament at 340.46 mg. (Drug + co-solvent = 50 mg + 290.46 mg)

Determining the weight of carrier material

It was calculated by using Eq. (4), by putting the value of W = 340.46 mg (weight of liquid medicament) and Lf = 1.5 (Liquid load factor) in it. The weight of required carrier material was found to be 226.97 mg. Determining the weight of coating material by using Eq. (1) the weight of the required coating material was calculated, it came to 15.37 mg.

Primary trial for selection of carrier and coating material.

The composition of liquisolid compact batch is given in Table 3. The quantities for labrasol, carrier material and coating material were taken as per calculation steps explained in the previous section. Sodium starch glycolate (SSG) as disintegrant (4% w/w) and Magnesium sterate (MgS) as a lubricant (1%w/w) were also added in the formulation. During preliminary trials it was observed that the neusilin /co rn starch ratio and R-value (carrier/coating material) had a significant effect on the drug release from the liquisolid compact, so it was decided to use 3^2 full factorial designs for determining the extent of their impact on the desired product characteristics. Table 1 displays the coded and transformed values for selected

Table 3:Composition of design batches for BRN liquisolid Compact.

CODE	BRN	Labrasol	Neusilin + CS	Aerosil 200	SSG (4%)	MgS (1%)	Total Weight
BLC-1	50	290.46	226.97 (204.27 + 22.69)	33.93	22.85	6.24	630.45
BLC- 2	50	290.46	226.97 (181.59+45.38)	33.93	22.85	6.24	630.45
BLC-3	50	290.46	226.97 (158.83+68.14)	33.93	22.85	6.24	630.45
BLC-4	50	290.46	226.97 (204.27 + 22.69)	22.62	22.69	6.17	623.83
BLC-5	50	290.46	226.97 (181.59+45.38)	22.62	22.69	6.17	623.83
BLC-6	50	290.46	226.97 (158.83+68.14)	22.62	22.69	6.17	623.83

BLC-7	50	290.46	226.97 (204.27 + 22.69)	11.31	21.14	5.99	605.87
BLC-8	50	290.46	226.97 (181.59+45.38)	11.31	21.14	5.99	605.87
BLC-9	50	290.46	226.97 (158.83+68.14)	11.31	21.14	5.99	605.87

* **All the weights are in mg.**

Preparation of BRN liquisolid compact

Fitting of data into the model:

In order to find out the best fit model, all the observed responses obtained for 9 formulations were concurrently fit into different mathematical models using Design-Expert® software. The selection of best fit model was based on the high values of multiple correlation coefficients (R^2), adjusted R^2, and predicted R^2 values and low values of standard deviation (SD), coefficients of variation (% CV), and predicted residual sums of the square (PRESS) (Table 4). The PRESS value indicates how well the model fits the data. The PRESS value for the chosen model should be small in comparison to the other models. The best fit model for percentage transmittance was quadratic model whereas it was linear model for self-emulsification time and percentage cumulative drug release.

Effect of independent variables on % drug release (Y_1) of BRN-LSC :

The % drug release of BRN-LST formulations are shown in table 1. The % drug release values were found in the range of 58.23 to 98.12 %. The effect of the independent variables on the % drug release can be described by the following quadratic equation.

$$Y_1 = + 88.07 + 6.76\ X_1 + 10.22X_2 - 1.66X_1X_2 + 0.73X_1^2 - 12.07X_2^2 \quad (1)$$

Where Y_1 is % drug release, X_1 is the carrier: coating ratio and X_2 is the neusilin : corn starch ratio. The equation indicates that carrier: coating ratio and neusilin: corn starch ratio has a positive effect on the % drug release. This demonstrates that % drug release of BRN-LSC increases with increase in the carrier: coating ratio and neusilin: corn starch ratio. The high coefficient value of X_2 specifies that the neusilin: corn starch ratio has more prominent effect on the % drug release of BRN-LSC compared to that of carrier: coating ratio. The ANOVA results for the % drug release data are shown in Table 5. The Model F-value of 35.62 implies the model is significant. There is only a 0.71% chance that a "Model F-Value" this large could occur due to noise. Values of "Prob > F" less than 0.0500 indicate model terms are significant. In this case X_1, X_2, X_2^2 are significant model terms. The Predicted R-Squared (R^2)" of 0.8060 is in reasonable agreement with the Adjusted R-Squared (R^2) of 0.9558. The adequate precision ratio of 17.646 indicates an adequate signal. Hence the quadratic model can be used to navigate the design space (Table 4).

Table 4. Regression analysis results obtained for various responses Y_1 (% drug release) and and Y_2 (disintegration time time) of BRN-LSC for fitting to different models

Models	SD	R^2	Adjusted R^2	Predicted R^2	PRESS	CV (%)	Remark
Response (Y_1)							
Linear	7.35	0.7356	0.6475	0.4282	700.54	9.13	
2FI	7.91	0.7446	0.5914	0.0259	1193.38	9.83	
Quadratic	2.60	0.9834	0.9558	0.8060	237.74	3.23	Suggested
Response (Y_2)							
Linear	2.95	0.9241	0.8988	0.8262	119.65	4.37	
2FI	3.16	0.9274	0.8838	0.6898	213.51	4.69	
Quadratic	1.44	0.9910	0.9760	0.9227	53.21	2.13	Suggested

SD: standard deviation, R^2: multiple correlation coefficient, 2FI: two factor interaction, PRESS: predicted residual sum of square, CV: coefficient of variation.

Table 5. ANOVA results for various responses of BRN-LSC

Source	Responses					
	Y_1 (% drug release)			Y_2 (disintegration time)		
	F-value	p-value Prob > F	Adequacy precision	F-value	p-value Prob > F	Adequacy precision
Model	35.62	0.0071	17.646	66.06	0.0029	23.865
X_1	40.53	0.0078		72.65	0.0034	
X_2	92.69	0.0024		235.37	0.0006	
X_1X_2	1.62	0.2922		1.09	0.3733	
X_1^2	0.16	0.7192		0.11	0.7644	
X_2^2	43.09	0.0072		21.09	0.0194	

X_1, and X_2 are coded terms for independent variables; X_1X_2 interaction terms; X_1^2 and X_2^2 are quadratic terms

The effects of the independent variables on the % drug release are represented by 3D- response surface graphs (Figure 1(A)) and their corresponding 2D- contour plots (Figure. 1(B)). It is noticeable from the graphs and the plots that the % drug release increased with increase in the carrier: coating ratio and neusilin: corn starch ratio. The perturbation plot (Figure 1(C)) for % drug release also supported these observations. The perturbation graph exhibits a slight bend for factor A (carrier: coating ratio) and a steep slope for factor B (neusilin: corn starch ratio) representing that the neusilin:corn starch ratio was a significant factor controlling the % drug release. [46]

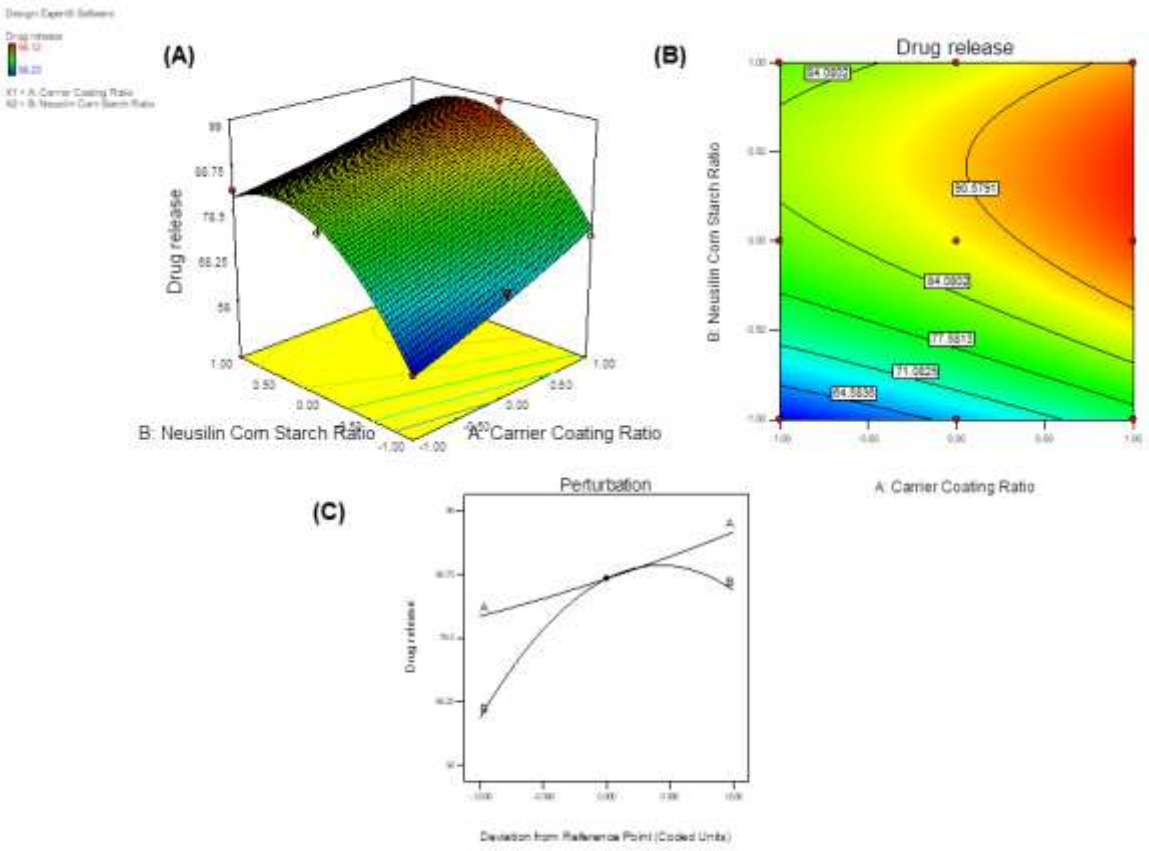

Figure 1. 3D-Response surface (A), 2D-contour (B) and perturbation plots (C) showing the effect of carrier: coating ratio and neusilin: corn starch ratio on % drug release of BRN-LTC.

Effect of independent variables on disintegration time (Y_2) of BRN-LTC:

The results of disintegration time of BRN-LSC formulations are shown in table 1. The disintegration time were found to be in the range of 58 to 84 seconds. The effect of the independent variables on the disintegration time can be explained by the following quadratic equation.

$$Y_2 = + 64.56 – 5.00\ X_1 – 9.00\ X_2 + 0.75\ X_1X_2 - 0.33\ X_1^2 + 4.67\ X_2^2 \qquad (2)$$

Where Y2 is disintegration time, X_1 is the carrier: coating ratio and X_2 is the neusilin : corn starch ratio. The equation indicates that carrier: coating ratio and neusilin : corn starch ratio has a negative effect on the disintegration time. This demonstrates that disintegration time of BRN-LSC decreases with increase in the carrier: coating ratio and neusilin : corn starch ratio. The high coefficient value of X_2 specify that the neusilin:corn starch ratio has more prominent effect on the disintegration time of BRN-LSC compared to that of carrier: coating ratio. The ANOVA results for the disintegration time data are shown in Table 5. The Model F-value of 66.06 implies the model is significant. There is only a 0.29% chance that a "Model F-Value" this large could occur due to noise. Values of "Prob > F" less than 0.0500 indicate model terms are significant. In this case X_1, X_2 and X_2^2 are significant model terms. The "Pred R-Squared" of 0.9227 is in reasonable agreement with the "Adj R-Squared" of 0.9760. The adequate precision ratio of 23.865 indicates an adequate signal (Table 4). Hence the linear model can be used to navigate the design space.

The 3D- response surface graphs and their corresponding 2D- contour plots showing the effects of the independent variables on the disintegration time are shown in figure 2. It is observed from the graphs and the plots that the disintegration time decreased with increase in the carrier: coating ratio and the neusilin: corn starch ratio. A perturbation plot can also provide an understanding about the effect of independent factors on responses. The perturbation plot (Figure 2(C) for disintegration time also supported the observations of 3D- response surface graphs and 2D- contour plots. [47]

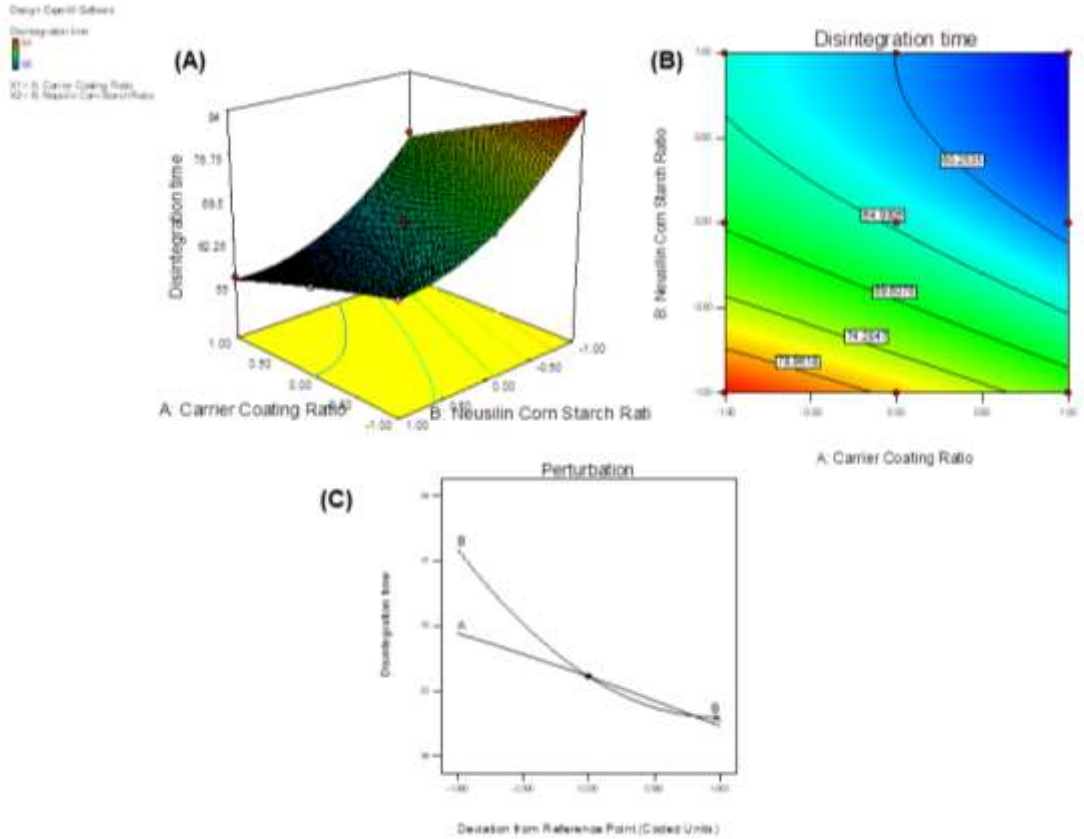

Figure 2. 3D-Response surface (A), 2D-contour (B) and perturbation plots (C) showing the effect of carrier: coating ratio and neusilin:corn starch ratio on disintegration time of BRN-LTC.

In order to find out the optimized formulation of BRN-LSC in the design space, numerical optimization process was carried out by applying constraints on the independent variables (% drug release - maximize; and disintegration time – minimize. This formula showed desirability value closer to unity (0.979). The overlay plot displays the optimized formulation along with their predicted response values (figure 3). The optimized BRN- LSC formulation was prepared and evaluated for the responses. The predicted and observed response values along with their % prediction error for the optimized formulation are shown in Table 6. The values were well in an agreement providing proof for successful design validity and optimization. The % prediction error values (-2.57 to 3.13) were well within the agreement demonstrating the validity of QbD design employed in the optimization of BRN-LSC.[48]

Table 6. Validation of optimized formulation

Response	Predicted value	Observed value	Prediction error (%)
% drug release	96.66	99.15	-2.57
Disintegration time (seconds)	56.13	54.37	3.13

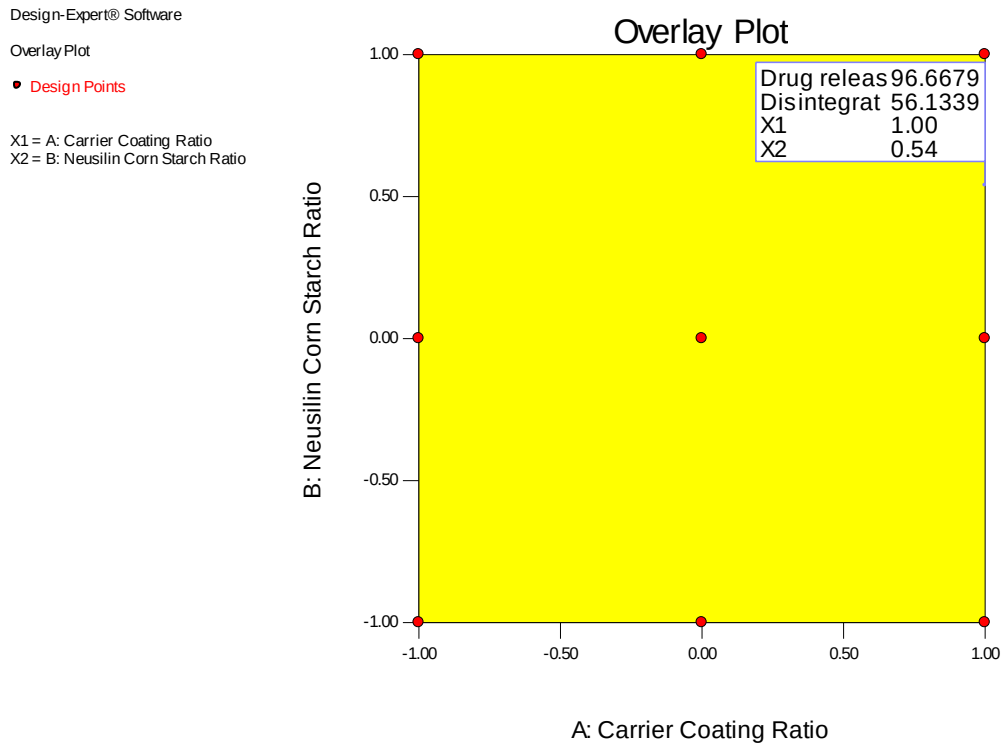

Figure 3: The overlay plot displaying the optimized BRN-LTS formulation in the design space and their predicted response values.

Drug-excipients compatibility study
FTIR

The FTIR spectral analysis was employed to ascertain compatibility between the BRN and excipients of raft system. The FTIR spectra of pure BRN, labrasol, neusilin US2 and BRN liquisolid compact are shown in Figure 1. FTIR spectra of BRN (Figure 4A), showed aromatic C–H at 3191.4 cm^{-1} C-H aliphatic at 2909.06 cm^{-1}, cyno group at (C-N) 1495.67 cm^{-1} , ether C-O-C stretch at 1100.77 cm^{-1} and OH stretching at 3318.3 cm^{-1} .

The FTIR spectra of BRN liquisolid compact (Figure 4D), showed functional groups peaks of showed OH stretching at 3314.71 cm^{-1} ,aromatic C–H at 3193.90 cm^{-1} C-H aliphatic at 2978.68 cm^{-1}, cyno group at (C-N) at 1497.72 cm^{-1} and ether C-O-C stretch at 1102.58 cm^{-1} respectively. The principal peaks of BRN are retained in the FTIR spectra of BRN liquisolid compact. Thus, obtained results clearly revealed compatibility (no chemical interaction) between BRN and formulation excipients of BRN liquisolid compact.[49]

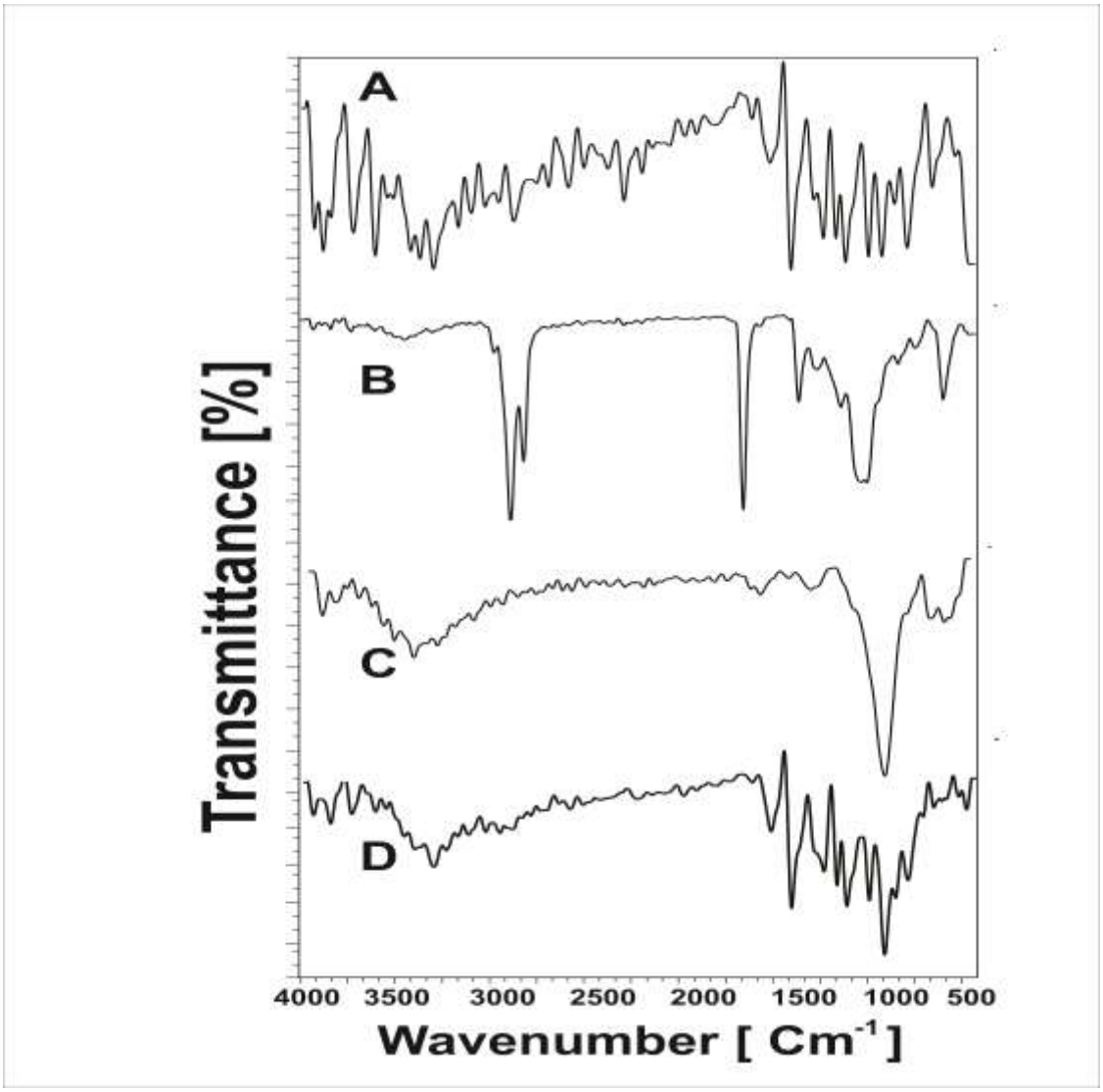

Figure 4. FTIR spectra of A) BRN B) Maisine C) Neusilin and D) BRN-LSC

DSC Studies

Differential scanning calorimetry is and unique tool utilized to ascertain compatibility between the BRN and formulation excipients of liquisolid tablet. The DSC thermo grams of plain BRN, labrasol,neusilin US2 and physical mixture of BRN and excipients of excipients of liquisolid tablet is shown in Figure 2. The DSC thermo gram of plain BRN (Figure 5A), and labrasol, (Figure 5B), and neusilin US2 showed peaks corresponding to BRN at 155.43 °C ,labrasol showed endothermic peak at 110.57°C and neusilin

US2 showed peak at 151.75°C.. On the other hand DSC thermo gram of physical mixture of BRN and excipients of liquisolid tablet (Figure 5C) endothermic peak observed at 157.82°C which is analogous to the peak of BRN. Thus, obtained results revealed that integrity of BRN was retained after combining with BRN liquisolid compact excipients which conforms compatibility of BRN with formulation excipients.[50]

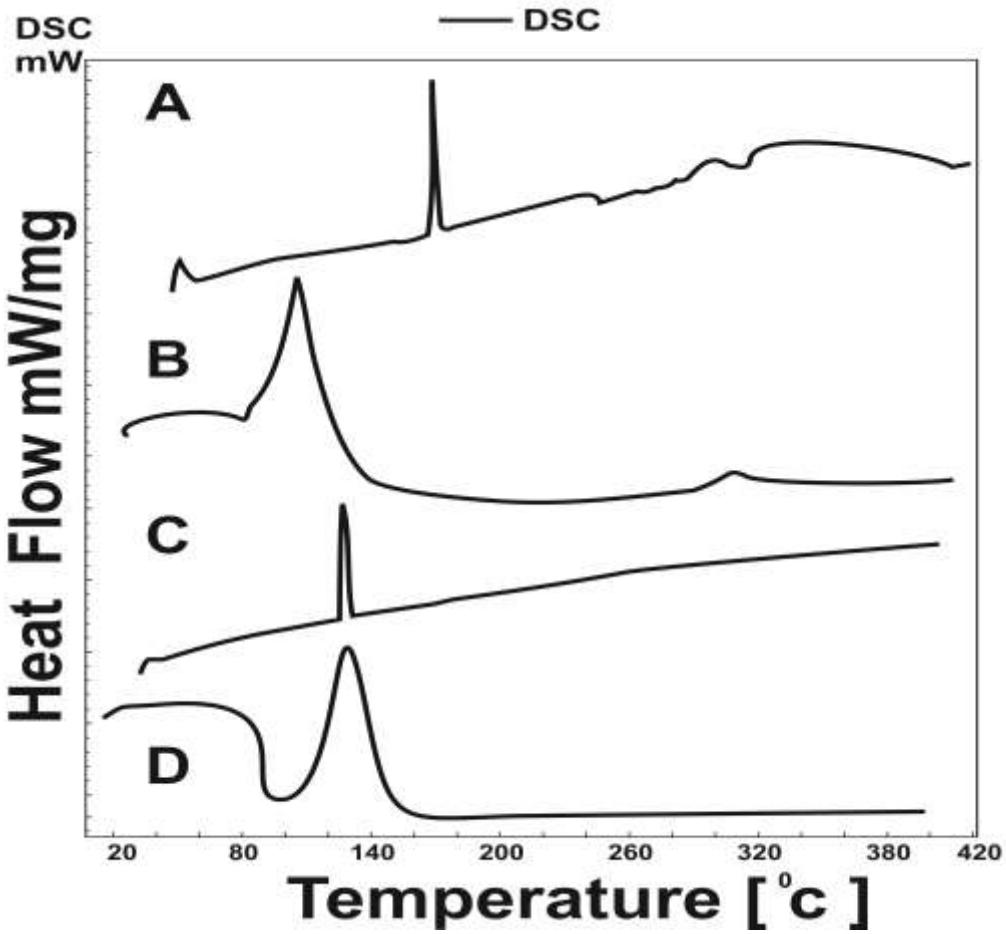

Figure 5. DSC thermo gram of A) BRN B) Labrasol C) Neusilin and D) BRN-LSC

Characterization of Solid-BRN liquisolid compacts

3.5.1. Micromeritic properties of optimized Optimizied BRN liquisolid compacts

The angle of repose of BRN–LSC 6 formulation was 30.42±0.25°, indicating good flow properties. BD and TD were found to be 0.3874± 0.040 g/mL and 0.4200± 0.027 g/mL respectively. CCI was found to be 3.28±0.19 %, while the HR was 1.105±0.078.

3.5.2. Post-compression parameters of BRN liquisolid compacts

Drug content, hardness, friability and weight variation of optimizied SGN liquisolid compact **(**BRN –LSC 6) was found to be 98.54±2.43%, 3.2± 0.78, 0.36±0.023 % and 623.83±1.75 mg respectively.

In-Silico Interaction Studies

Molecular docking was performed to explore the putative binding mode and interactions of Berberine with Neusilin excipient using AutoDock4.2.1. The least binding energy conformation of Berberine , with Neusilin were found to be -5.34 kcal/mol, as shown in Figure 6. The docking analysis reveals that Berberine, binds with Neusilin and stabilized by the bonding and non-bonding interactions. The Neusilin-Berberine complex shows the hydrogen bonding interactions of Neusilin OH with O3 residue of

Berberine (2.17 Å) and pi-type of non-bonded interaction between Neusilin with Berberine (4.30 Å) as shown in Figure 6. The analysis of results shows that the complex is stabilized by the classical hydrogen bonding and CH type of bonding, also non-bonding interactions contributes equally.[23]

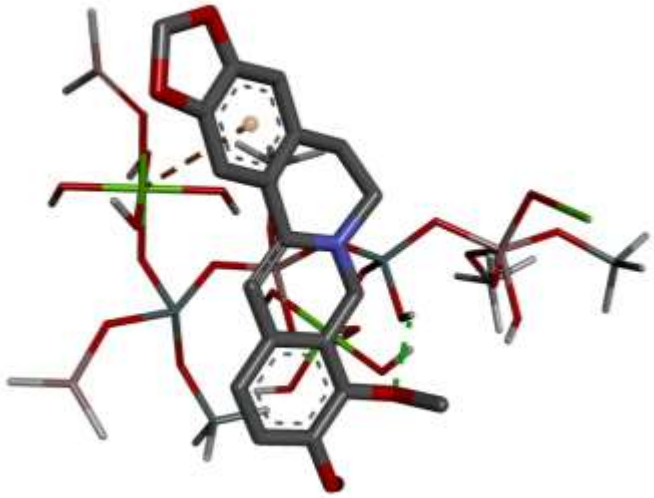

Figure 6: Interaction of Berberine with Neusilin excipient using molecular docking. Here, the carbon atoms of Berberine and Neusilin are shown in the cyan color. While, Hydrogen, Oxygen, Nitrogen, Aluminum, Magnesium, and Silicon are shown in white, red, blue, bricks, green, and grey colors, respectively.

In vitro Antidiabetic Study

α-amylase inhibitory Assay

Alpha-amylase activity can be measured in-vitro by hydrolysis of starch in the presence of α-amylase enzyme. Due to its major role in the breakdown of polysaccharides, alpha-amylase is considered one of the most important enzymes in the digestion process found primarily in the saliva and pancreatic juice. Targeting this enzyme and inhibiting it is one of the possible solutions to prevent high postprandial blood glucose [51-52]. Alpha-amylase inhibition potential of BRN, BRN-LSC and acarbose is demonstrated in Figure 7. The calculated IC_{50} showed that BRN-LSC inhibition potential is nearly matches with standard acarbose, with an IC_{50} of 8.14 ± 0.42 mg/mL noted for SGN-LST against 7.61 ± 0.35 mg/mL noted for acarbose. On the other hand SGN showed IC_{50} of 16.38 ± 0.63. The reduced values of IC_{50} of BRN-LSC indicates the better enzyme-induced hydrolysis of starch into monosaccharide which directly proportional to the α-amylase inhibitory activity.

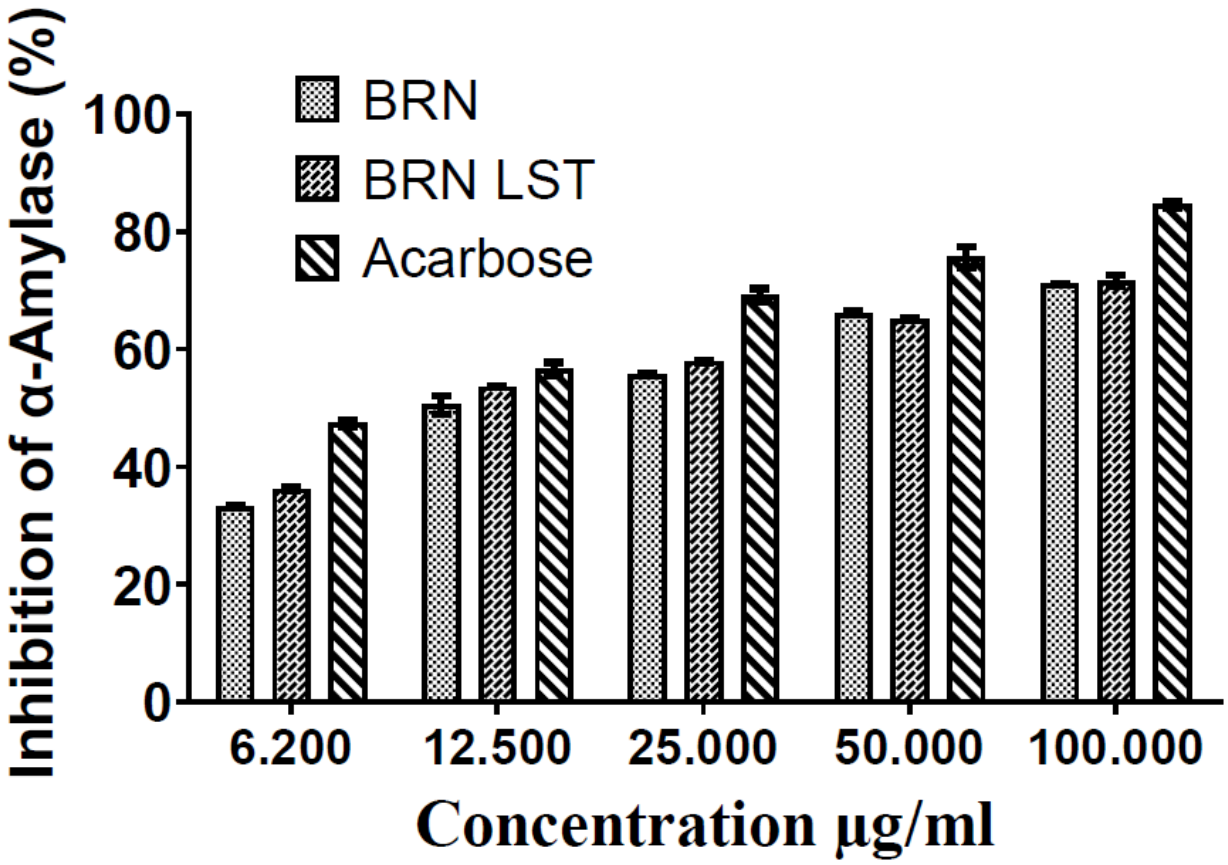

Figure 7. Alpha-amylase inhibition potential of BRN, BRN-LSC and acarbose

α-Glucosidase inhibition assays

Alpha-Glucosidase Inhibitory Effect The α-glucosidase enzyme is also one of the essential enzymes of the digestion, located in the mucosal brush border of the small intestine.In type 2 DM, inhibition of α-glucosidase therapy is beneficial to delay absorption of glucose after a meal.α-glucosidase plays a role in the conversion of carbohydrates into glucose. By inhibiting α-glucosidase, glucose levels in the blood can be returned within normal which may probably suppress the diabetes progression [43]**.** Figure 8 demonstrate α-glucosidase inhibition of activity of BRN, BRN-LSC and acarbose. The calculated IC_{50} showed that the inhibition potential of BRN-LSC (IC_{50} 6.18 ± 0.37) is better than that of SGN (IC_{50} 12.63.11 ± 0.49) which quite similar to standard acarbose (IC_{50} 4.93 ± 0.13 mg/mL)

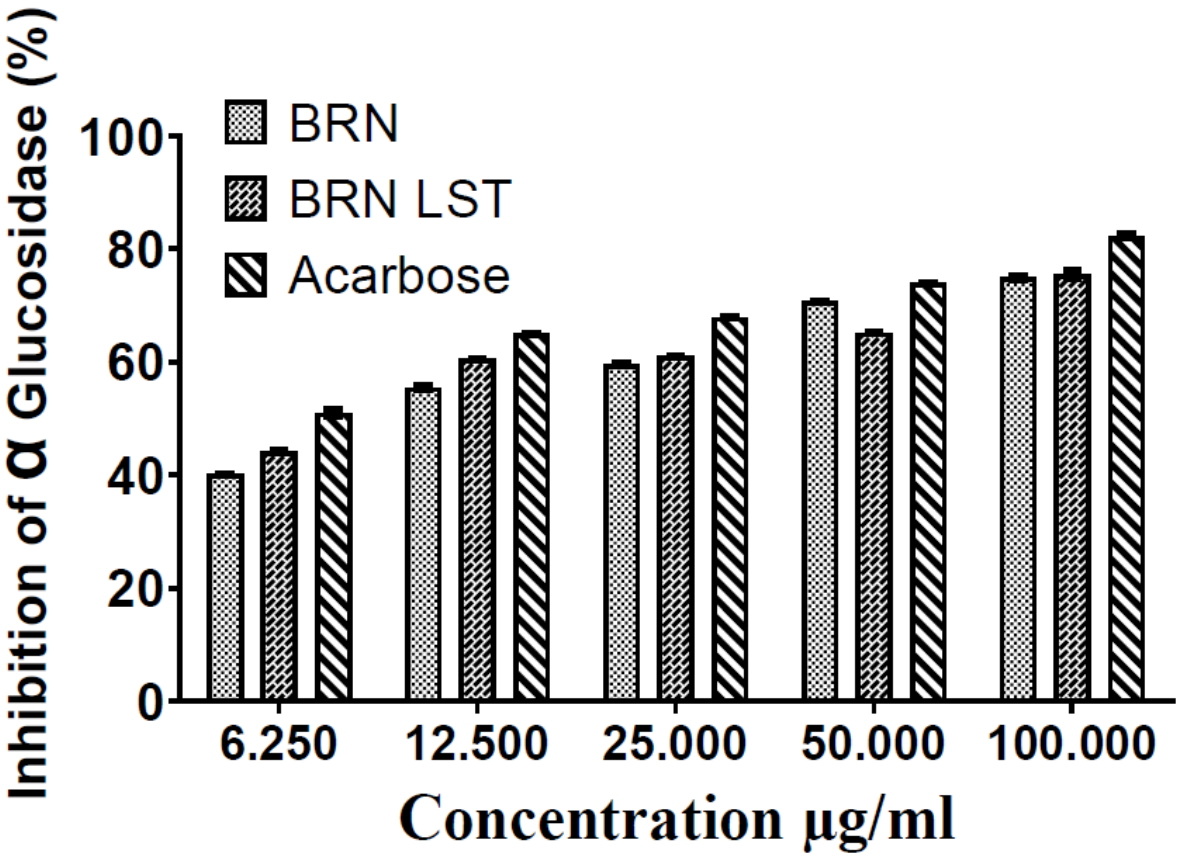

Figure 8. *α*-glucosidase inhibition of activity of BRN, BRN-LSC and acarbose

In Vivo Pharmacokinetic Study:

The retention time of BRN in plasma was found to be 5.10 min. As can be seen in plasma concentration vs. time profiles (Figure 9), C_{max} determined after administration of BRN liquisolid compact was found to be 70.09±6.38 ng /mL, attained at 2 h, whilst, C_{max} for pure BRN (12.27±2.34 ng mL−1) was reached at 1 h (T_{max}). Plasma concentration obtained after administration of liquisolid compact was significantly higher ($P < 0.05$) than plain BRN, at all studied time points. Significantly higher ($P < 0.05$) AUC was obtained for BRN liquisolid compact (447.77±35.29 ng.h.mL−1) than plain BRN (54.93±4.79 ng.h.mL−1). For BRN liquisolid compact and BRN elimination half-life ($T_{1/2}$) was found to be 7.83±0.82 & 3.01±0.34 hours respectively. Mean residence time (MRT) for BRN liquisolid compact and BRN was found to be 8.07±0.79 & 4.80±0.42 hours respectively. [53-54] Detailed results are shown in Table 7.

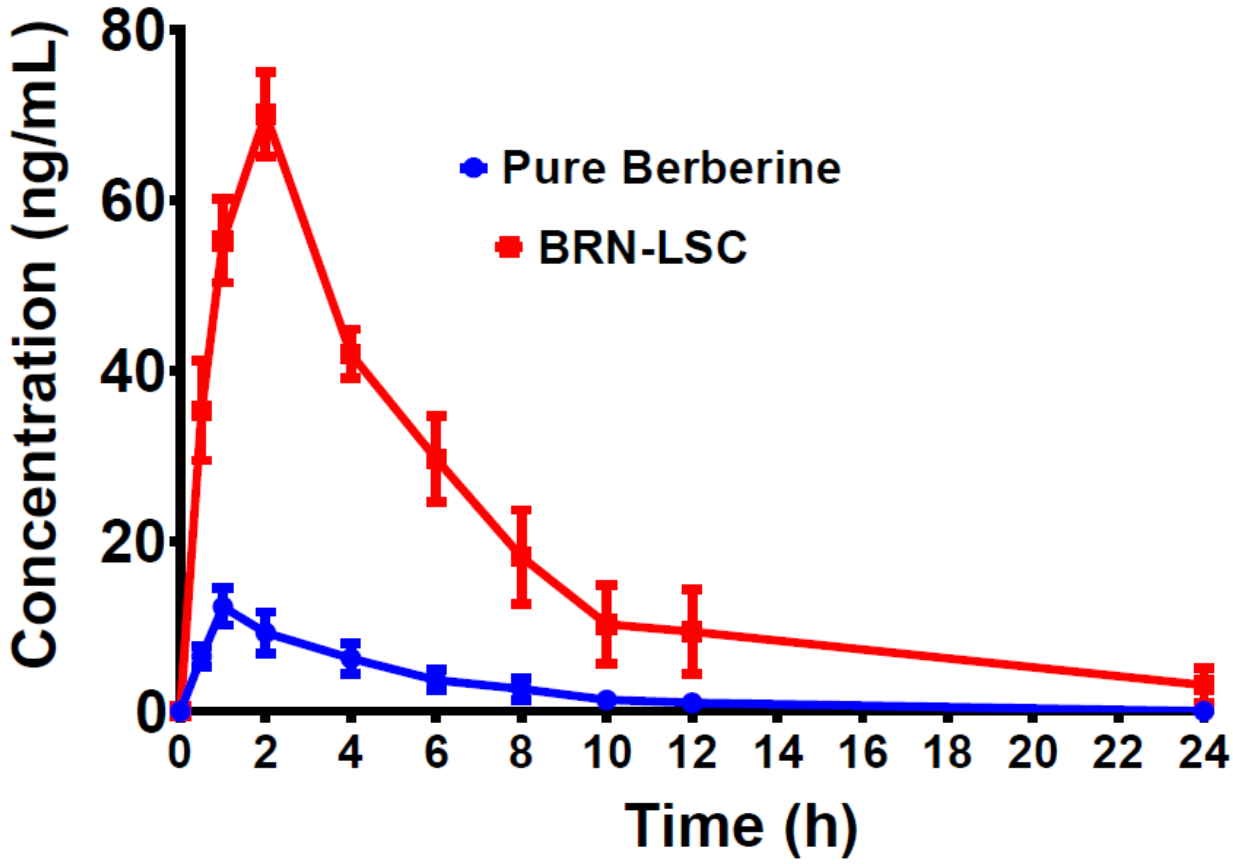

Figure 9. In-vivo Pharmacokinetic study of BRN and BRN-LSC after 24 hours in albino wistar rats.

Table 7:Pharmacokinetic Parameters of barberine (BRN) after oral administration of BRN and BRN LSC formulation (5 mg/kg) in rats.

Parameter	BBN	BRN-LSC
T_{max} (h)	1	2
C $_{max}$ (ng/ml)	12.27±2.34	70.09±6.38
AUC (ng/ml*h)	54.93±4.79	447.77±35.29
AUMC (ng/ml*h^2)	284.88±26.54	3894.20±72.63
$t_{1/2}$ (h)	3.01±0.34	7.83±0.82
MRT (h)	4.80±0.42	8.07±0.79
CL (mg)/(ng/ml)/h	0.084	0.010
Relative Bioavailability		815.16

Stability Study

A stability study of optimized BRN-LSC for 03 months at accelerated conditions of RH and temp. 40 °C & 75% ± 5% was performed to check the influence of storage conditions on cumulative drug release and disintegration time of optimized BRN-LSC. No significant change ($p>0.5$) was noted in the characteristics of liquisolid compact during the storage period. Detailed results are reported in Table 8.

Table 8: Accelerated Stability Study Data of BRN Liquisolid compact for 03 Months period

Parameter	Initial	1 Month	2 Month	3 Month
CDR (%)	98.76±0.36	98.62±0.42	98.53±0.34	98.42±0.27
Disintegration Time (Sec.)	58.57±1.35	58.23±1.49	57.52 ±2.32	57.41±2.25

All values represent mean ± standard deviation (n=3)

Conclusion:

In the present study, labrasol based BRN liquisolid compact were successfully prepared and optimized using a factorial design approach. Optimized BRN liquisolid compact was evaluated for numerous in–vitro and in–vivo parameters. The design batches have acceptable compact properties such as flow property, compactibility, hardness, friability, content uniformity and disintegration time. The design batches had significantly high dissolution rate compared to pure drug-containing tablets at all the defined time intervals. The results of DSC studies suggested that the improved dissolution profile of liquisolid compact was possibly either due to the drug being in an amorphous state or molecularly dispersed in the liquisolid compact. Loading of BRN in liquisolid compact escalated the solubility of BRN, in vitro antidiabetic efficacy and bioavailability to a greater extent. Conclusively, BRN liquisolid compact would be a promising approach for BRN to improve its therapeutic interventions.

CONFLICT OF INTEREST

The authors declare that they don't have any competing interests.

ACKNOWLEDGEMENTS

The authors are thankful to Department of Pharmacy, Vels University Chennai, and Tamilnadu for providing required guidance and support for completion of present research work.

AUTHORS' CONTRIBUTIONS

MD research scholar who contributed in design and characterization of SGN liquisolid tablet and MD has major contributors in writing the manuscript, EB supervisors who contributed in research guidance and has major contribution in monitoring antidiabetic studies and discussion. All authors read and approved the final manuscript.

References

1. Mobasseri M, Shirmohammadi M, Amiri T, Vahed N, Hosseini Fard H, Ghojazadeh M. Prevalence and incidence of type 1 diabetes in the world: a systematic review and meta-analysis. Health Promot Perspect. 2020 Mar 30;10(2):98-115. doi: 10.34172/hpp.2020.18.
2. Lin, X., Xu, Y., Pan, X. et al. Global, regional, and national burden and trend of diabetes in 195 countries and territories: an analysis from 1990 to 2025. Sci Rep 10, 14790 (2020). https://doi.org/10.1038/s41598-020-71908-9.
3. Pradeepa, Rajendra; Mohan, Viswanathan. Epidemiology of type 2 diabetes in India. Indian Journal of Ophthalmology: November 2021 - Volume 69 - Issue 11 - p 2932-2938 doi: 10.4103/ijo.IJO_1627_21.
4. Divers J, Mayer-Davis EJ, Lawrence JM, et al. Trends in Incidence of Type 1 and Type 2 Diabetes Among Youths— Selected Counties and Indian Reservations, United States, 2002–2015. MMWR Morb Mortal Wkly Rep. 2020 Feb 14;69(6):161–165.
5. Spiras S, Bolton SM, Liquisolid systems and methods for preparing same, United States patent 5,1999,968,550.
6. Bertocchi P, Antoniella E, Valvo L, Diclofenac sodium multisource prolonged release tablets- a comparative study on the dissolution profiles, J Pharm and biomedical analysis, 2005;37:679-685.
7. Spireas S, Jarowski CI, Rohera BD, Powdered solution technology: principles and mechanism, Pharm. Res, 1992; 9 (10):1351–1358.
8. Lobenberg R, Amidon, GL. Modern bioavailability, bioequivalence and biopharmaceutics classification system; new scientific approaches to international regulatory standards. Eur J Pharm Biopharm, 2000; 50: 3–12.
9. Darwish AM., Dissolution enhancement of glibenclamide using liquisolid tablet technology, Acta Pharm, 2001; 51: 173-181.

10. Manisha Khemani, Maheshwar Sharon, and Madhuri Sharon. Encapsulation of Berberine in Nano-Sized PLGA Synthesized by Emulsification Method. International Scholarly Research Network.Nanotechnology.2012, 1-9. doi:10.5402/2012/187354.
11. Sahibzada MUK, Sadiq A, Faidah HS, Khurram M, Amin MU, Haseeb A, Kakar M. Berberine nanoparticles with enhanced in vitro bioavailability: characterization and antimicrobial activity. Drug Des Devel Ther. 2018 Feb 14;12:303-312. doi: 10.2147/DDDT.S156123.
12. Duong TT, Isomäki A, Paaver U, Laidmäe I, Tõnisoo A, Yen TTH, Kogermann K, Raal A, Heinämäki J, Pham TM. Nanoformulation and Evaluation of Oral Berberine-Loaded Liposomes. Molecules. 2021 Apr 29;26(9):2591. doi: 10.3390/molecules26092591.
13. Patel VP, Patel NM, Dissolution enhancement of glipizide using liquisolid tablet technology, Ind Drugs, 2008; 45(4): 318-323.
14. Fahmy RH, Kassem MA. Enhancement of famotidine dissolution rate through liquisolid tablet formulation: in vitro and in vivo evaluation, Eur J Pharm Biopharm, 2008; 69(3):993-1003.
15. Jaydip B, Dhaval M, Soniwala MM, Chavda J. Formulation and optimization of liquisolid compact for enhancing dissolution properties of efavirenz by using DoE approach. Saudi Pharm J. 2020 Jun;28(6):737-745. doi: 10.1016/j.jsps.2020.04.016.
16. Naveen Chella, Nataraj Narra, Tadikonda Rama Rao, "Preparation and Characterization of Liquisolid Compacts for Improved Dissolution of Telmisartan", Journal of Drug Delivery, vol. 2014, 10 pages, 2014. https://doi.org/10.1155/2014/692793.
17. Patel DS, Pipaliya RM, Surti N. Liquisolid Tablets for Dissolution Enhancement of a Hypolipidemic Drug. Indian J Pharm Sci. 2015 May-Jun;77(3):290-8. doi: 10.4103/0250-474x.159618.
18. Patel, H., Gupta, N., Sonia, P., & Ranch, K. (2019). Development of liquisolid tablets of chlorpromazine using 32 full factorial design. Indian Journal of Pharmaceutical Sciences, 81(6), 1107-1114.
19. Cirri M, Mura P, Valleri M, Brunetti L. Development and Characterization of Liquisolid Tablets Based on Mesoporous Clays or Silicas for Improving Glyburide Dissolution. Pharmaceutics. 2020; 12(6):503. https://doi.org/10.3390/pharmaceutics12060503.
20. Ahmed TA, Alotaibi HA, Alharbi WS, Safo MK, El-Say KM. Development of 3D-Printed, Liquisolid and Directly Compressed Glimepiride Tablets, Loaded with Black Seed Oil Self-Nanoemulsifying Drug Delivery System: In Vitro and In Vivo Characterization. Pharmaceuticals (Basel). 2022 Jan 5;15(1):68. doi: 10.3390/ph15010068.
21. Barbora Vraníková, Jan Gajdziok & Petr Doležel (2017) The effect of superdisintegrants on the properties and dissolution profiles of liquisolid tablets containing rosuvastatin, Pharmaceutical Development and Technology, 22:2, 138-147, DOI: 10.3109/10837450.2015.1089900.
22. Patel T, Patel LD, Suhagia BN, Soni T, Patel T. Formulation of fenofibrate liquisolid tablets using central composite design. Curr Drug Deliv. 2014;11(1):11-23. doi: 10.2174/15672018113109990051.
23. Sunil T. Galatage, Rahul Trivedi, Durgacharan A. Bhagwat,Oral self-emulsifying nanoemulsion systems for enhancing dissolution, bioavailability and anticancer effects of camptothecin,Journal of Drug Delivery Science and Technology,Volume 78,2022,https://doi.org/10.1016/j.jddst.2022.103929.
24. Spireas S, Sadu S, Grover R. In vitro release evaluation of hydrocortisone liquisolid tablets, J Pharm Sci, 1998; 87: 867-872.
25. Elkordy, A.A., Tan, X.N., Essa, E.A., 2013. Spironolactone release from liquisolid formulations prepared with CapryolTM 90, Solutol HS-15 and Kollicoat SR 30 D as non-volatile liquid vehicles. Eur. J. Pharm. Biopharm. 83, 203–223.
26. Tayel, S.A., Soliman, I.I., Louis, D., 2008. Improvement of dissolution properties of carbamazepine through application of the liquisolid tablet technique. Eur. J. Pharm. Biopharm. 69, 342–347.
27. Spireas, S., 2002. Liquisolid systems and methods of preparing same. Google Patents.
28. Javadzadeh, Y., Jafari-Navimipour, B., Nokhodchi, A., 2007. Liquisolid technique for dissolution rate enhancement of a high dose water-insoluble drug(carbamazepine). Int. J. Pharm. 341, 26–34.
29. S. T. Galatage, S. G. Killedar, R. B. Katakar, R. B. Kumbhar, M. Sharma, P. J. Shirote, Development and Characterization of Floating Tablets of Nizatidine for Peptic Ulcer, Journal of Advances in Medical and pharmaceutical sciences,21(2019),1-12.
30. S.T Galatage.Development and characterization of microparticles of sumatriptan succinate drug carrier system via nasal route,International Journal of Pharmaceutical Sciences and Research 2019;10:(9),4194-4200.
31. Galatage ST, Manjappa AS, Kumbhar PS, Salawi A, Sabei FY, Siddiqui AM, Patil RV, Akole VS, Powar RD, Kagale MN. Synthesis of silver nanoparticles using Emilia sonchifolia plant for treatment of bloodstream diseases caused by Escherichia coli. Ann Pharm Fr. 2022 Dec 15:S0003-4509(22)00179-1. doi: 10.1016/j.pharma.2022.12.007.
32. Galatage ST, Trivedi R, Bhagwat DA. Characterization of camptothecin by analytical methods and determination of anticancer potential against prostate cancer. Future Journal of Pharmaceutical science.2021May7;104:1-9. doi.org/10.1186/s 43094- 021- 00236-0.
33. D. A. Bhagwat,P.A.Swami,S.J.Nadaf,P.B. Choudhari,V.M. Kumbar, H.N. More, S.G.Killedar, P.S. Kawtikwar, Capsaicin Loaded Solid SNEDDS for Enhanced Bioavailability and Anticancer Activity: In-Vitro, In-Silico, and In-Vivo Characterization, J. Pharm.(2021)
34. G.M.Morris, H. Ruth, W. Lindstrom, M.F. Sanner, R.K. Belew, D.S. Goodsell, A.J. Olson, Software news and updates AutoDock4 and AutoDockTools4: Automated docking with selective receptor flexibility, J. Comput. Chem, 30(2006),2785–2791.
35. Kumbhar, V.V. Bhandare, Exploring the interaction of Peloruside-A with drug-resistant αβII and αβIII tubulin isotypes in human ovarian carcinoma using a molecular modeling approach, J. Biomol. Struct. Dyn,(2020).
36. B.V.Kumbhar, V.V. Bhandare, D. Panda, A.Kunwar, Delineating the interaction of combretastatin A-4 with αβ tubulin isotypes present in drug-resistant human lung carcinoma using a molecular modeling approach, J. Biomol. Struct. Dyn, 38 (2020).
37. A. Rai, Gupta, T.K, Kini, S.A. Kunwar, A. Surolia, D. Panda, CXI-benzo-84 reversibly binds to tubulin at colchicine site and induces apoptosis in cancer cells, Biochem. Pharmacol, 86 (2013), 378–391.
38. J.B.Venghateri, T.K. Gupta, P.J. Verma, A. Kunwar, D.Panda, Ansamitocin P3 depolymerizes microtubules and induces apoptosis by binding to tubulin at the vinblastine site, PLoS One 8, e75182 (2013).
39. W.L. DeLano, The PyMOL Molecular Graphics System, Schrödinger LLC (2003).

40. Patil SM,Galatage ST,Choudhari AU.Evelopment Of Uv Spectrophotometric Method For Estimation Of Letrozole In Pure And Pharmaceutical Dosage Form. Indo American Journal of Pharmaceutical Research.2018 May;8(04):1080-1085.
41. Galatage ST, Hebalkar AS,Killedar SG (2020).Design and Characterization of camptothecin gel for the treatment of epidermoid carcinoma.Future journal of pharmaceutical sciences.2020,6:50;1-11.
42. K. Y. Kim, K. A. Nam, H. Kurihara, and S.M. Kim, "Potent α- glucosidase inhibitors purified from the red alga Grateloupia elliptica," Phytochemistry, vol. 69, no. 16, pp. 2820–2825, 2008.
43. L. H. Bosenberg and D. G. Van Zyl, "The mechanism of action of oral antidiabetic drugs: a review of recent literature," Journal of Endocrinology, Metabolism and Diabetes of South Africa, vol. 13, no. 3, pp. 80–88, 2008.
44. M,R.Peram ,S. Jalalpure,V. Kumbar,S. Patil,S. Joshi,K. Bhat,P. Diwan Factorial design based curcuminethosomalnanocarriers for the skin cancer delivery: in vitro evaluation,Journal of liposome research, 29 (2019), 291-311.
45. Kottke, M., Chueh, H.-R., Rhodes, C., 1992. Comparison of disintegrant and binder activity of three corn starch products. Drug Dev. Ind. Pharm. 18, 2207–2223.
46. Spireas S, Sadu S. Enhancement of prednisolone dissolution properties using liquisolid compacts. Int J Pharm, 1998; 166: 177-188.
47. Javadzadeh Y, Shariati H, movahhed-danesh E, Effects of different grades of microcrystalline cellulose on flowability, compressibility and dissolution of liquisolid systems, Drug DevInd Pharm,2008;1-9 .
48. Akhtar Rasul, Safirah Maheen, Hafeez Ullah Khan, Maria Rasool, Shahid Shah, Ghulam Abbas, Khurram Afzal, Fatima Tariq, Irum Shahzadi, Muhammad Hassham Hassan Bin Asad, "Formulation, Optimization, In Vitro and In Vivo Evaluation of Saxagliptin-Loaded Lipospheres for an Improved Pharmacokinetic Behavior", BioMed Research International,. 2021, 1-17 https://doi.org/10.1155/2021/3849093.
49. Alhamhoom Y, Ravi G, Osmani RAM, Hani U, Prakash GM. Formulation, Characterization, and Evaluation of Eudragit-Coated Saxagliptin Nanoparticles Using 3 Factorial Design Modules. Molecules. 2022 Nov 3;27(21):7510. doi: 10.3390/molecules27217510.
50. Nitin S. Desai, Sunil T. Galatage , Swapnil S. Harale , Suresh G. Killedar. Design And Characterization Of Aceclofenac Bionanocomposite Using Natural Solubilizers.IJPSR, 2021; Vol. 12(12): 1000-12.
51. Sunil T.Galatage, S.G.Killedar, D.A.Bhagwat, J.K.Saboji. Development and Characterization of Microsponge of Amphotercin B for Topical Drug Delivery. Research Journal of Pharmaceutical, Biological and Chemical Sciences 10 .2019.
52. Li T, Zhang XD, Song YW. A microplate-based screening method for alphaglucosidase inhibitors. Chinese Chin J Clin Phamaco Ther. 2005;10:1128–34.
53. Kodoli, R.S., Galatage, S.T., Killedar, S.G. et al. Hepatoprotective activity of Phyllanthus niruri Linn. endophytes. Futur J Pharm Sci 7, 97 (2021). https://doi.org/10.1186/s43094-021-00243-1.
54. Rasul A, Maheen S, Khan HU, Rasool M, Shah S, Abbas G, Afzal K, Tariq F, Shahzadi I, Asad MHHB. Formulation, Optimization, In Vitro and In Vivo Evaluation of Saxagliptin-Loaded Lipospheres for an Improved Pharmacokinetic Behavior. Biomed Res Int. 2021 Oct 20;2021:3849093. doi: 10.1155/2021/3849093.